Low-energy fusion of doubly magic nuclei: The notable case of $^{16}O + ^{48}Ca$

A. M. Stefanini,[1] G. Montagnoli,[2,3] M. Del Fabbro,[2,3] F. Fontana,[3] P. Aguilera,[2] G. Andreetta,[1,3] D. Brugnara,[1] G. Colucci,[4] L. Corradi,[1] E. Fioretto,[1] F. Galtarossa,[2] A. Goasduff,[1] B. Gongora Servin,[1,3] A. Gozzelino,[1] M. Heine,[5] G. Harmant,[5] D. Mengoni,[2,3] M. Luciani,[6] K. Rezynkina,[2,3] S. Rocca,[1,3] and D. Stramaccioni[1,3]

[1]*INFN, Laboratori Nazionali di Legnaro, I-35020 Legnaro, Italy*
[2]*INFN, Section of Padua, I-35131 Padua, Italy*
[3]*University of Padua, I-35131 Padua, Italy*
[4]*Heavy Ion Laboratory, University of Warsaw, 02-093 Warszawa, Poland*
[5]*Université de Strasbourg, CNRS, IPHC UMR 7178, 67000 Strasbourg, France*
[6]*INFN Section and University of Milan, I-20133 Milan, Italy*

(Received 7 April 2025; accepted 29 May 2025; published 20 June 2025)

Background: Near- and sub-barrier fusion reactions between doubly magic nuclei are important benchmarks for theoretical models to reproduce the experimental excitation functions. Here we consider the cases of $^{16}O + ^{16}O$, $^{48}Ca + ^{48}Ca$, and $^{16}O + ^{208}Pb$, which have been measured previously, as well as $^{40}Ca + ^{90}Zr$, even though $Z = 40$ is not a major shell closure.
Purpose: We aim to perform a complete measurement of the excitation function of $^{16}O + ^{48}Ca$, to investigate its behavior near and below the Coulomb barrier where no data are available. Qualitative considerations suggest that this case should follow a trend similar to the other doubly magic systems. However, this might be disproved by the experiment, due to the very large positive fusion Q value and/or to the possible existence of hindrance with a high energy threshold.
Methods: The experiment was performed at the XTU Tandem of Laboratori Nazionali di Legnaro INFN. 24–42 MeV ^{16}O beams, with intensities up to 20 p nA, and ^{48}Ca targets of 50 $\mu g/cm^2$ were used. The evaporation residues (ER) were detected by the electrostatic deflector setup PISOLO at forward angles, and identified by their energy and two independent times of flight, between the final Si detector and two microchannel plate (MCP) detectors.
Results: The clear separation of the evaporation residues in the *E*-ToF (time-of-flight) spectra allowed the excitation function to be measured down to $\sigma_{fus} \sim 2$ μb. The results were compared with coupled-channels (CC) calculations using the Akyüz-Winther potential, and a small sub-barrier fusion enhancement was observed. We extracted the logarithmic derivative of the excitation function and the astrophysical *S* factor, as well as the fusion barrier distribution where a single peak is observed, as predicted by the CC calculations. Comparing with other investigated doubly magic systems reveals an analogous behavior down to the lowest measured energies.
Conclusions: The *S* factor develops a maximum vs energy, and the logarithmic derivative reaches the so-called L_{CS} value, at the rather high cross section $\simeq$0.8 mb. This is evidence of the fusion hindrance phenomenon whose threshold follows the phenomenological systematics established for medium-light systems. A large positive Q value for fusion does not play a role in the $^{16}O + ^{48}Ca$ system. The CC model is able to reproduce the excitation function down to that point. At lower energies the fusion cross sections are consistent with the one-dimensional barrier tunneling limit. In the spirit of the adiabatic model, decreasing (and vanishing) coupling strengths reproduce the cross sections far below the barrier, while the hindrance model fails in that energy region.

DOI: 10.1103/hj5x-r1gw

I. INTRODUCTION

The study of nuclei with closed-shell numbers of both protons and neutrons (doubly magic nuclei) has been, and continues to be, very important for unveiling a number of nuclear structure properties connected to the shell model. Analogously, near- and sub-barrier fusion reactions [1,2] between such nuclei are important starting points for theoretical models trying to reproduce the experimental evidences. The systems in which fusion excitation functions have been measured near the barrier are $^{16}O + ^{16}O$ (see Ref. [3] and several other articles cited, e.g., in [1]), $^{48}Ca + ^{48}Ca$ [4], and $^{16}O + ^{208}Pb$ [5]. We may consider also $^{40}Ca + ^{90}Zr$ [6] even though $Z = 40$ is not a major shell closure.

As expected, a limited sub-barrier cross section enhancement is observed for the light system $^{16}O + ^{16}O$. The enhancement increases for the heavier ones. The phenomenon of hindrance [7] shows up in $^{48}Ca + ^{48}Ca$ and $^{16}O + ^{208}Pb$, while its existence in $^{16}O + ^{16}O$ is still controversial also because of the different low-energy trends observed in several measurements for that system. The onset of hindrance is observed at the lowest energies also in $^{40}Ca + ^{90}Zr$ [8].

A few other doubly magic systems are not considered in this article for various reasons, even though rather complete sets of fusion data exist: (1) $^{48}Ca + ^{208}Pb$ [9] leads in the region of superheavy nuclei and it involves different dynamical features (e.g., quasifission); (2) for $^{40}Ca + ^{48}Ca$ [10] two-neutron transfer largely influences the sub-barrier cross sections; (3) in the case of $^{40}Ca + ^{40}Ca$ [11] the cross sections were measured only above $\simeq$20 μb, probably preventing the observation of hindrance.

Considering the extensive investigations on sub-barrier fusion reported in literature starting from the 1980s, it is quite surprising that no relevant data are available for $^{16}O + ^{48}Ca$. Recall that a basic difference between heavy- and light-ion systems is the sign of the fusion Q value (Q_{fus}). For $^{16}O + ^{48}Ca$, Q_{fus} is as large as +18.14 MeV. Note that experimental data are available for the "twin" system $^{16}O + ^{40}Ca$ [12] only far above the barrier ($\sigma_{fus} \geqslant 470$ mb).

These considerations and the evidence of Ref. [13] may suggest that the fusion excitation function of $^{16}O + ^{48}Ca$ will follow a trend similar to the other doubly magic systems. However, this might be disproved by experiment, possibly due to the very large positive fusion Q value and/or to the possible existence of hindrance with a high energy threshold, as observed in the medium-light case $^{24}Mg + ^{12}C$ [14], a situation still not reproduced by theoretical models.

According to the estimate of the phenomenological analysis of Ref. [1], the hindrance threshold of $^{16}O + ^{48}Ca$ is expected to be around $E_{c.m.} = 18.8$ MeV ($E_{lab} = 25$ MeV). We note that few-nucleon transfer Q values are all large and negative for this system, apart from two-proton stripping ($Q = -0.55$ MeV). It follows that only coupling to α stripping ($Q = +0.52$ MeV) might enhance the low-energy fusion cross section to a significant extent.

We found it attractive to measure the fusion excitation function of this doubly magic $^{16}O + ^{48}Ca$ system from well below to above the Coulomb barrier, since its behavior will constitute a missing benchmark for current models of the hindrance phenomenon. The sudden model of hindrance implies a repulsive core in the interaction due either to the nuclear incompressibility [15] or to the Pauli exclusion principle [16]. On the other hand, the adiabatic model [17,18] suggests that the coupling strengths should decrease to zero, especially near the point of contact between nuclei. This is due to the transition from a two-body potential to a one-body potential in the overlap region.

Note that the experimental uncertainties in the S factor at low energies in the $^{24}Mg + ^{12}C$ [14] reaction did not discriminate between calculations based on the sudden and adiabatic models. Our purpose has been to clarify this point by an experiment on $^{16}O + ^{48}Ca$ with smaller statistical errors and reaching the lowest possible cross section. Furthermore, observing hindrance in $^{16}O + ^{48}Ca$, and thereby determining its energy and cross section thresholds, will enable a more reliable extrapolation to the light systems relevant for astrophysics.

This paper is organized as follows: after this Introduction, Sec. II illustrates the experimental setup and the method used to obtain the fusion cross sections. In Sec. III we present the results of coupled-channels (CC) calculations. We also compare these results with the astrophysical S factor and the logarithmic derivative of the excitation function, extracted from the data. The following Sec. IV is dedicated to the fit of low-energy cross sections using an empirical approach and the hindrance model. In Sec. V the present data are compared with those other doubly magic systems, and in Sec. VI we update the phenomenological systematics of hindrance threshold for medium-light systems. Section VII summarizes and concludes this article.

II. EXPERIMENT

The experiment was performed at the XTU Tandem accelerator of the INFN–Laboratori Nazionali di Legnaro, using ^{16}O beams with intensities up to 20 pnA, in the energy range 24–42 MeV. Thin targets of 50 μg/cm^2 $^{48}CaF_2$ were employed, evaporated on a 10 μg/cm^2 carbon layer. The isotopic enrichment of ^{48}Ca was $\simeq$97% in mass 48. The small contamination by lower-mass stable calcium isotopes in the target had a negligible effect on the fusion cross sections due to higher Coulomb barriers in the laboratory system. The fusion-evaporation residues (ER) were detected and identified at 2°–3° forward angles, using the LNL electrostatic beam deflector setup. A detector telescope installed downstream, consisting of two microchannel plates (MCP) followed by a silicon detector, measured the ER energy and two times of flight (ToF).

Four silicon detectors were used for beam control and normalization between the different runs by measuring the Rutherford scattering. They were placed above and below, and to the left and right of the beam at the same scattering angle $\theta_{lab} = 20.3^o$ (for more details see Ref. [19]).

The ER angular distribution was measured at $E_{beam} = 30$ MeV covering the θ_{lab} range from $-6°$ to $+8°$. The angular distribution was fit with a Gaussian curve (see Fig. 1). By integrating the angular distribution, the ratio of the yield at $\theta_{lab} = 2°$ (3° at the lower energies) to the total ER yield was obtained (see Ref. [6]). No significant variation with energy of the width of the angular distribution is expected in the measured energy range, as observed in previous measurements (see, e.g., Refs. [20,21]). This was confirmed by pace4 calculations [22] performed for the present system across the measured energy range. Therefore, the same Gaussian width was employed for all energies where the fusion cross section was measured only at $\theta_{lab} = 2°$ (3°).

The relative errors on the cross sections are determined by the statistical uncertainties ($\approx$2% near and above the barrier and larger, up to 50%, at the lowest energies). The absolute error on the cross-section scale was estimated to be ±7–8% [19]. The lowest measured cross section is 2.8 ± 1.45 μb and an upper limit $\sigma \leqslant 2.4$ μb was determined for the lowest energy, $E_{beam} = 24.25$ MeV. The measured excitation function is shown in Fig. 2, and the corresponding cross sections are listed in Table I.

III. COUPLED-CHANNELS CALCULATIONS

The present data were analysed with the CC code ccfull [23]. The calculations were performed using the standard

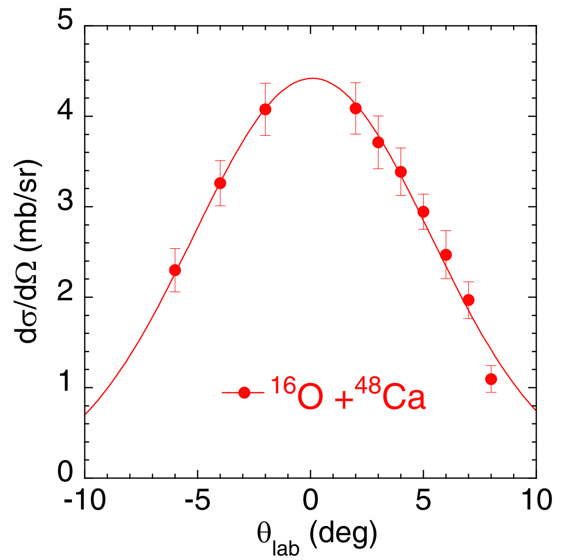

FIG. 1. ER angular distribution measured for $^{16}O + ^{48}Ca$ at $E_{lab} = 30$ MeV, together with a Gaussian fit. Only statistical errors are reported. The full line is the Gaussian fit to the data, having a width (standard deviation) $\sigma = (5.25 \pm 0.17)^{\circ}$.

TABLE I. Fusion cross sections of $^{16}O + ^{48}Ca$ measured in this work. Statistical uncertainties are quoted, while the absolute cross section scale is estimated to be accurate within ±7%. We indicate with E the center-of-mass energy.

E (MeV)	σ (mb)	E (MeV)	σ (mb)
18.20	$\leqslant$0.00024	23.82	112.4 ± 3.5
18.57	0.0028 ± 0.0015	24.57	178.3 ± 5.8
18.94	0.0055 ± 0.0039	25.32	253 ± 6
19.32	0.016 ± 0.009	26.07	311 ± 7
20.07	0.213 ± 0.059	26.82	370 ± 8
20.44	0.467 ± 0.092	27.57	436 ± 9
20.82	1.30 ± 0.19	28.32	506 ± 10
21.57	6.19 ± 0.51	29.07	542 ± 10
22.32	21.7 ± 1.3	29.82	597 ± 10
23.07	60.8 ± 2.0	30.57	697 ± 12
		31.32	733 ± 13

Akyüz-Winther parametrization of the ion-ion potential [24], with a well depth $V_0 = 52.34$ MeV, radius parameter $r_o = 1.17$ fm, and diffuseness $a = 0.63$ fm. The resulting Coulomb barrier is $V_b = 23.0$ MeV in the center-of-mass (c.m.) frame. ^{16}O is considered inert since its lowest excitations lie above 6 MeV. The lowest quadrupole and octupole excitations of ^{48}Ca were included in the CC calculations, and the coupling parameters are reported in Table II.

The CC calculations well reproduce the data down to $\sigma \simeq 0.8$ mb, and the cross-section enhancement with respect to the no-coupling calculation is small, as expected for the present medium-light and stiff system. Nevertheless, one can note that the CC results start overestimating the experimental data below that cross section (see Fig. 2), even though the effect is limited. That is the point where the hindrance phenomenon shows up.

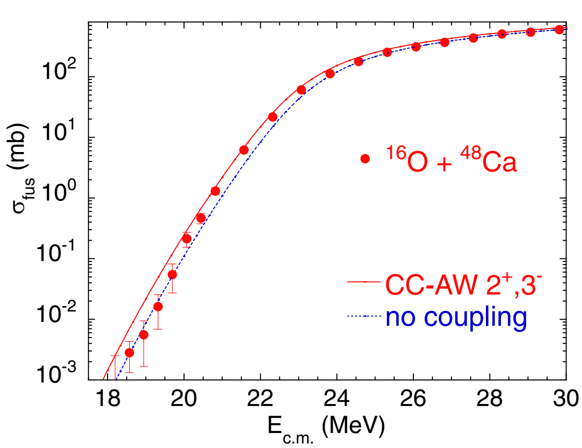

FIG. 2. Fusion excitation function of $^{16}O + ^{48}Ca$ measured in this work.

It is interesting to note that the lowest 4–5 energy points agree with the no-coupling limit. This behavior is similar to what was observed for the two lighter systems $^{12}C + ^{24}Mg$, ^{30}Si [14,21]; however, in the present case, the evidence is beyond doubt (see Fig. 4, top panel).

The small statistical errors on the cross sections allowed us to obtain the fusion barrier distribution that is shown in Fig. 3 (top panel). Its shape is essentially that of a single barrier, with evidence of a further small peak at energies higher than the main one. The CC calculations give a good account of the data. We note that the couplings produce a small shift toward low energies with respect to the no-coupling result, without any change of shape. The small peak(s) showing up at high energies might be due to inelastic/mutual excitations not included in the coupling scheme.

The bottom panel of Fig. 3 shows the logarithmic derivative (slope) of the energy-weighted excitation function, approximated by the incremental ratio using every other experimental point, with an energy step $\Delta E_{c.m.} = 0.75$ MeV (1.5 MeV in the higher energy range). One sees that, with decreasing energy, the data trend is a steady increase up to the L_{CS} value (evidence of hindrance), followed by a decline at the very lowest energies. The same panel of Fig. 3 shows, however, that the CC calculations are not able to reproduce this behavior of the low-energy derivative.

We also extracted the astrophysical S factor from the measured cross sections. This is reported in Fig. 4, bottom panel, together with the CC and no-coupling results. The ordinate is

TABLE II. Excitation energies E_x, spin and parities λ^{π}, reduced transition probabilities, and deformation parameters β_{λ} [25,26] for the lowest quadrupole and octupole modes of ^{48}Ca. The β_{λ} values are obtained using the radius parameter $r_0 = 1.20$ fm, and nuclear and Coulomb deformation parameters were taken to be the same.

Nucleus	E_x (MeV)	λ^{π}	$B(E\lambda)\uparrow$ (W.u.)	β_{λ}
^{48}Ca	3.832	2^+	1.79(60)	0.106(3)
	4.507	3^-	9(2)	0.235(1)

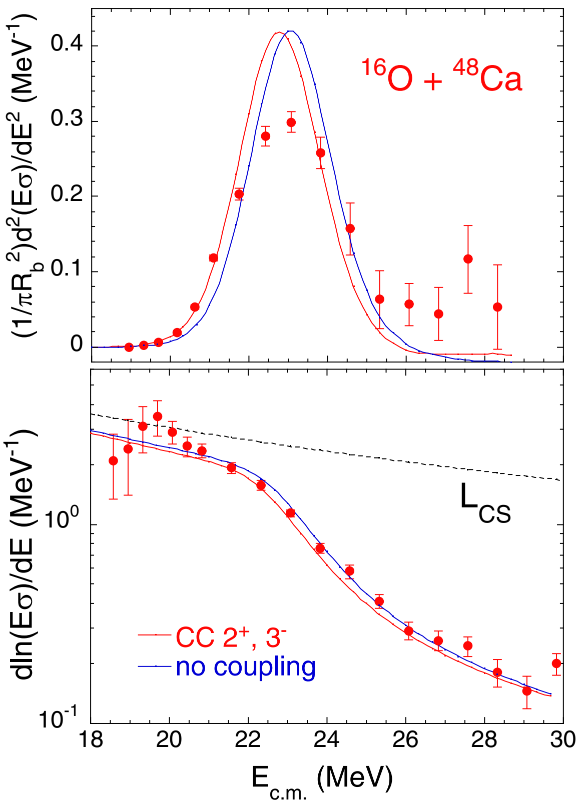

FIG. 3. Fusion barrier distribution (top panel), and logarithmic derivative of the excitation function of $^{16}O + ^{48}Ca$ (bottom panel), compared to the results of CC calculations described in the text.

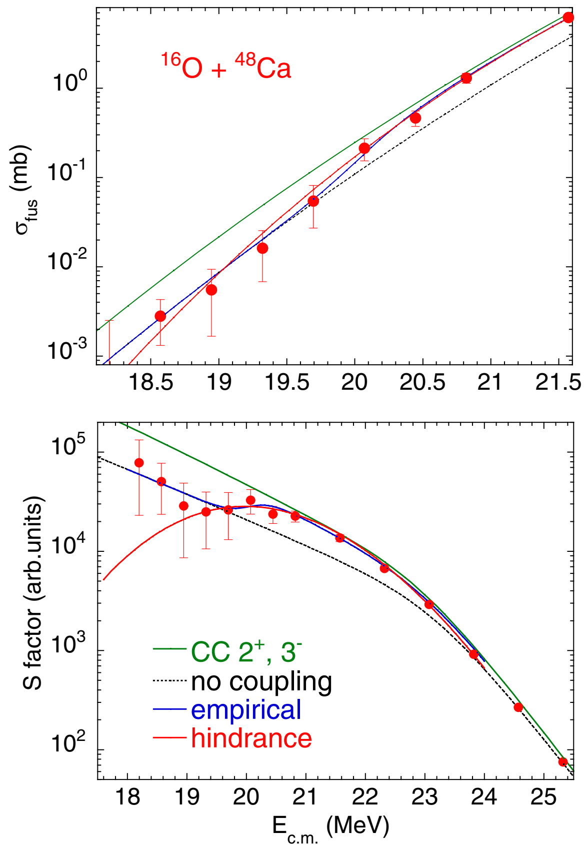

FIG. 4. Low-energy part of the excitation function (upper panel), and astrophysical S factor (bottom panel) for $^{16}O + ^{48}Ca$. Here the upper limit at $E = 18.20$ MeV is not plotted. The data are compared to the results of CC calculations described in the text.

given by

$$S(E) = \sigma(E)E\exp[2\pi(\eta - \eta_o)],$$

where $\eta_o = 18$ is a suitable constant scaling the S factor. The low-energy S factor values mirror the behavior of the excitation function, and make it quite clear that the lowest fusion points follow the no-coupling calculation.

As a summary of the CC results based on the AW potential and presented in this section, we note that they give a good account of the fusion cross sections and of the barrier distribution, as well of the slope and S factor down to the point where the hindrance phenomenon shows up. At lower energies, the cross sections and consequently the S factor are consistent with one-dimensional barrier penetration predictions, and neither CC nor no-coupling results are able to reproduce the particular trend of the logarithmic slope. Thus, we have adopted a more phenomenological approach, employing two different models to fit the experimental evidence at the lowest energies. This is described and discussed in the next section.

IV. FITTING THE LOW-ENERGY TRENDS

Following the approach outlined in Ref. [14], we fitted the low-energy cross sections using an empirical function $\beta(E)$. This function simulates the damping of coupling strengths below the barrier in accordance with the adiabatic model [17,18,27]

$$\ln[\sigma_{\rm exp}(E)] = \beta(E)\ln[\sigma_{\rm CC}(E)] + [1 - \beta(E)]\ln[\sigma_{\rm noc}(E)]. \quad (1)$$

The behavior of the excitation function suggests that $\beta(E)$ should approach unity near the barrier and zero at low energies. We therefore interpolated its trend vs energy with a smooth Fermi function (see again Ref. [14]),

$$\beta(E) = \frac{1}{1 + \exp[\alpha_o(E - E_o)]}. \quad (2)$$

We derived $\beta(E)$ values for each measured energy using both the data points and the ccfull calculations (discussed in the previous section). The interpolation yields $\alpha_o = -4.995$ MeV^{-1} and $E_o = 20.064$ MeV. Using these values, $\beta(E)$ was obtained for all energies, and, consequently, the fusion cross section results were obtained from Eq. (1). This, in turn, has given us the empirical S factor curve in the bottom panel of Fig. 4.

The interpolating curve shows a good fit with the measured cross sections. That curve transitions from the CC results to the no-coupling limit as energy decreases. This transition produces a maximum in the S factor (shown in the bottom

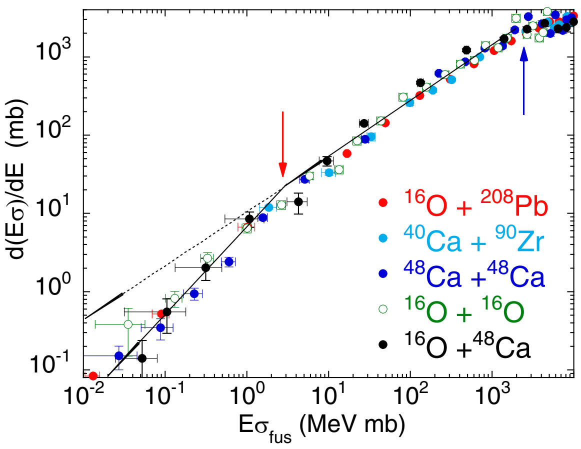

FIG. 5. Two-dimensional plot $d(E\sigma)/dE$ vs $E\sigma$ for $^{16}O + {}^{48}Ca$ and other doubly magic systems (see text for detailed comments). The full and dashed lines are drawn to guide the eye.

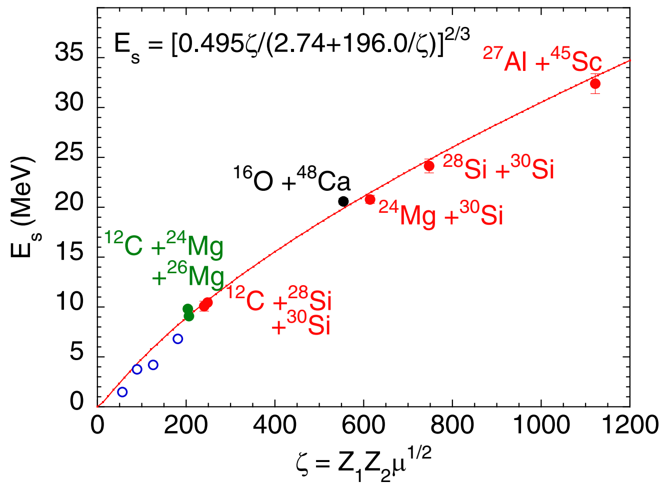

FIG. 6. Threshold energies for hindrance in light systems (updated from Ref. [29]). The uncertainties on some of the reported points are smaller than the symbol size. The system studied in the present work is represented by a black dot. The open symbols at low ζ values are obtained by extrapolating from higher energies, using the hindrance model (see Ref. [1]). They represent, with increasing ζ, $^{10}B + {}^{10}B$, $^{12}C + {}^{12}C$, $^{12}C + {}^{16}O$, and $^{16}O + {}^{16}O$.

panel of Fig. 4, blue line). Notably, the S factor increases again at the lowest energies, following the no-coupling calculation, as discussed in the preceding section. So, we observe evidence of gradual damping of the coupling strengths, and this behavior qualitatively aligns with the fundamental concept of the adiabatic model [17,18,27].

Alternatively, we have fitted the low-energy part of the excitation function using the expression derived by the hindrance model [28],

$$\sigma(E) = \frac{\sigma_s E_s}{E} \exp\left(A_o(E - E_s) - \frac{2B_o}{\sqrt{E_s}}\left[\sqrt{\frac{E_s}{E}} - 1\right]\right), \quad (3)$$

where A_o and B_o are the fit parameters, $E_s = 20.6$ MeV is the hindrance energy threshold, and $\sigma_s = 0.8$ mb is the corresponding cross section. The fit yielded $A_o = -7.04$ MeV^{-1} and $B_o = 898.8$ MeV$^{1/2}$.

The results of this fit are shown in the two panels of Fig. 4 (red line). As in the previous empirical approach, we obtain a good fit of the low energy excitation function with a clear maximum of the S factor. However, the increase of the S factor at the lowest energies is very clear and not reproduced, at variance with the case of $^{12}C + {}^{24}Mg$ [14] where the rather large experimental uncertainties do not allow one to distinguish between the two model fits in that energy range. The present data on $^{16}O + {}^{48}Ca$ allow us to discriminate between the two approaches. Furthermore, as pointed out in the previous section, the CC calculation (green line) does not show any S factor maximum, and the low-energy points are overpredicted.

V. COMPARISON WITH OTHER DOUBLY MAGIC SYSTEMS

The data for the present $^{16}O + {}^{48}Ca$ case and the other doubly magic systems cited in the Introduction are reported in Fig. 5, in the spirit of the recent Ref. [13], where the first energy derivative $d(E\sigma)/dE$ is plotted vs the energy-weighted excitation function $E\sigma$. In this representation, the Coulomb barrier height differences between the various systems are removed to a large extent. The data sets for all systems are very close to each other, as one expects since the colliding nuclei are very stiff. The sign of the fusion Q value does not have any significant influence, and couplings to transfer channels surely play marginal roles.

The blue arrow approximately marks the $E\sigma$ value of the highest barrier for all systems. Above that point, the derivative $d(E\sigma)/dE$ is essentially constant and equals πR_b^2, where R_b is the barrier radius according to the classical formula [13]. The red arrow is placed where a slope change of the derivatives trend can be observed, indicating the position of the lowest barrier. The $E\sigma$ range between the two arrows, therefore, indicates the total width of the fusion barrier distribution. The full and dashed lines in Fig. 5 are drawn to guide the eye.

VI. SYSTEMATICS

It is useful to recall that, several years ago, an empirical formula was developed to reproduce the energy threshold of hindrance for medium-mass stiff systems [29] and successfully applied also to lighter cases with negative and positive fusion Q value.

In recent years, further medium-light systems have been investigated ($^{12}C + {}^{24,26}Mg$, ^{30}Si), including the $^{16}O + {}^{48}Ca$ case, which is the object of the present study, and $^{12}C + {}^{28}Si$, whose study was recently completed [30] (see Fig. 6).

The threshold energies of these reactions were added to those reported in Ref. [29] and the overall systematic variation was refitted, thus obtaining a formula with updated parameters, which is reported in the figure.

The fitted line is a good representation of the thresholds for all investigated systems and for $^{16}O + {}^{48}Ca$. For the light cases of astrophysical interest, we see that the present updated fitted line predicts hindrance thresholds slightly higher than what was previously extrapolated.

VII. SUMMARY AND CONCLUSION

We measured the fusion excitation function of $^{16}O + ^{48}Ca$ from above to far below the barrier at Laboratory National di Legnaro, motivated by the peculiar nature of the system where both colliding nuclei are magic.

We used the ^{16}O beams from the XTU Tandem accelerator of LNL. The fusion-evaporation residues were detected and identified by an *E*-ToF telescope at 2°–3° forward angles downstream of an electrostatic beam deflector setup, consisting of two MCP detectors and one Si detector. The fusion cross sections could be measured down to a few μb.

CC calculations were performed using the Aküz-Winther potential, including the lowest 2^+ and 3^- excitations of ^{48}Ca. A good account of the data is obtained; however, the measured cross sections are over-predicted by the CC results below $\sigma_{\rm fus} \approx 0.8$ mb, which represents the hindrance threshold.

We point out that, at lower energies, the data are consistent with a pure one-dimensional tunneling (no coupling) calculation, as possibly observed for $^{12}C + ^{24}Mg$, ^{30}Si [14,21].

The excitation function is well fit using an empirical approach simulating the weakening of the coupling strengths at low energies, as indicated by the adiabatic model. The hindrance model reproduces the hindrance phenomenon, but it is not able to fit the *S* factor increase at the lowest energies.

In a comparison with other doubly magic systems investigated in previous years, the present case $^{16}O + ^{48}Ca$ does not show significant differences, when the various Coulomb barrier heights are properly taken into account.

We show that, when accounting for the trend of the present system and of other medium-light cases investigated in recent years, the phenomenological systematics proposed for heavier stiff systems several years ago [29] requires adjusting the relevant fit parameters, thus leading to updated predictions of the hindrance threshold for the light systems of astrophysical interest.

ACKNOWLEDGMENTS

We acknowledge the very professional work of the XTU Tandem staff for beam production and delivery, and of M. Loriggiola for preparing targets of excellent quality. The research leading to these results received funding from the European Union's Horizon 2020 research and innovation program under Grant Agreement No. 654002. G.H. acknowledges the Interdisciplinary Thematic Institute QMat, as part of the ITI 2021–2028 program of the University of Strasbourg, CNRS and Inserm, supported by IdEx Unistra (ANR 10 IDEX 0002), by the SFRI STRAT'US project (ANR 20 SFRI 0012), and by EUR QMAT ANR-17-EURE-0024 under the framework of the French Investments for the Future Program.

DATA AVAILABILITY

The data supporting this study's findings are available within the article.

[1] C. L. Jiang, B. B. Back, K. E. Rehm, K. Hagino, G. Montagnoli, and A. M. Stefanini, Heavy-ion fusion reactions at extreme subbarrier energies, Eur. Phys. J. A **57**, 235 (2021).

[2] G. Montagnoli and A. M. Stefanini, Recent experimental results in sub- and near-barrier heavy ion fusion reactions (2nd edition), Eur. Phys. J. A **59**, 138 (2023).

[3] J. Thomas, Y. T. Chen, S. Hinds, K. Langanke, D. Meredith, M. Olson, and C. A. Barnes, Sub-barrier fusion of ^{16}O with ^{16}O, Phys. Rev. C **31**, 1980 (1985).

[4] A. M. Stefanini, G. Montagnoli, R. Silvestri, L. Corradi, S. Courtin, E. Fioretto, B. Guiot, F. Haas, D. Lebhertz, P. Mason, F. Scarlassara, and S. Szilner, How does fusion hindrance show up in medium-light systems? The case of $^{48}Ca + ^{48}Ca$, Phys. Lett. B **679**, 95 (2009).

[5] M. Dasgupta, D. J. Hinde, A. Diaz-Torres, B. Bouriquet, C. I. Low, G. J. Milburn, and J. O. Newton, Beyond the coherent coupled channels description of nuclear fusion, Phys. Rev. Lett. **99**, 192701 (2007).

[6] H. Timmers, D. Ackermann, S. Beghini, L. Corradi, J. He, G. Montagnoli, F. Scarlassara, A. Stefanini, and N. Rowley, A case study of collectivity, transfer and fusion enhancement, Nucl. Phys. A **633**, 421 (1998).

[7] C. L. Jiang, H. Esbensen, K. E. Rehm, B. B. Back, R. V. F. Janssens, J. A. Caggiano, P. Collon, J. Greene, A. M. Heinz, D. J. Henderson, I. Nishinaka, T. O. Pennington, and D. Seweryniak, Unexpected behavior of heavy-ion fusion cross sections at extreme sub-barrier energies, Phys. Rev. Lett. **89**, 052701 (2002).

[8] A. M. Stefanini, G. Montagnoli, H. Esbensen, P. Čolović, L. Corradi, E. Fioretto, F. Galtarossa, A. Goasduff, J. Grebosz, F. Haas, M. Mazzocco, N. Soić, E. Strano, and S. Szilner, New results in low-energy fusion of $^{40}Ca + ^{90,92}Zr$, Phys. Rev. C **96**, 014603 (2017).

[9] H. W. Gäggeler, D. Jost, A. Türler, P. Armbruster, W. Brüchle, H. Folger, F. Heßberger, S. Hofmann, G. Münzenberg, V. Ninov, W. Reisdorf, M. Schädel, K. Sümmerer, J. Kratz, U. Scherer, and M. Leino, Cold fusion reactions with ^{48}Ca, Nucl. Phys. A **502**, 561 (1989).

[10] C. L. Jiang, A. M. Stefanini, H. Esbensen, K. E. Rehm, L. Corradi, E. Fioretto, P. Mason, G. Montagnoli, F. Scarlassara, R. Silvestri, P. P. Singh, S. Szilner, X. D. Tang, and C. A. Ur, Fusion hindrance for Ca plus Ca systems: Influence of neutron excess, Phys. Rev. C **82**, 041601(R) (2010).

[11] G. Montagnoli, A. M. Stefanini, C. L. Jiang, H. Esbensen, L. Corradi, S. Courtin, E. Fioretto, A. Goasduff, F. Haas, A. F. Kifle, C. Michelagnoli, D. Montanari, T. Mijatovic, K. E. Rehm, R. Silvestri, P. P. Singh, F. Scarlassara, S. Szilner, X. D. Tang, and C. A. Ur, Fusion of $^{40}Ca + ^{40}Ca$ and other Ca plus Ca systems near and below the barrier, Phys. Rev. C **85**, 024607 (2012).

[12] D. F. Geesaman, C. N. Davids, W. Henning, D. G. Kovar, K. E. Rehm, J. P. Schiffer, S. L. Tabor, and F. W. Prosser, Search for structure in the fusion of $^{16}O + ^{40}Ca$, Phys. Rev. C **18**, 284 (1978).

[13] A. M. Stefanini, G. Montagnoli, M. D. Fabbro, L. Corradi, E. Fioretto, and S. Szilner, The slopes of sub-barrier heavy-ion

fusion excitation functions shed light on the dynamics of quantum tunnelling, Sci. Rep. **14**, 12849 (2024).

[14] G. Montagnoli, A. M. Stefanini, C. L. Jiang, K. Hagino, F. Niola, D. Brugnara, P. Colovic, G. Colucci, L. Corradi, R. Depalo, E. Fioretto, A. Goasduff, G. Pasqualato, F. Scarlassara, S. Szilner, and I. Zanon, Fusion of $^{12}C + {}^{24}Mg$ at extreme sub-barrier energies, J. Phys. G **49**, 095101 (2022).

[15] H. Esbensen and S. Misicu, Hindrance of $^{16}O + {}^{208}Pb$ fusion at extreme sub-barrier energies, Phys. Rev. C **76**, 054609 (2007).

[16] C. Simenel, A. S. Umar, K. Godbey, M. Dasgupta, and D. J. Hinde, How the Pauli exclusion principle affects fusion of atomic nuclei, Phys. Rev. C **95**, 031601(R) (2017).

[17] T. Ichikawa, K. Hagino, and A. Iwamoto, Existence of a one-body barrier revealed in deep subbarrier fusion, Phys. Rev. C **75**, 057603 (2007).

[18] T. Ichikawa, Systematic investigations of deep sub-barrier fusion reactions using an adiabatic approach, Phys. Rev. C **92**, 064604 (2015).

[19] A. M. Stefanini, G. Montagnoli, L. Corradi, S. Courtin, E. Fioretto, A. Goasduff, F. Haas, P. Mason, R. Silvestri, P. P. Singh, F. Scarlassara, and S. Szilner, Fusion hindrance for $^{58}Ni + {}^{54}Fe$, Phys. Rev. C **82**, 014614 (2010).

[20] G. Montagnoli, A. M. Stefanini, H. Esbensen, C. L. Jiang, L. Corradi, S. Courtin, E. Fioretto, A. Goasduff, J. Grebosz, F. Haas, M. Mazzocco, C. Michelagnoli, T. Mijatovic, D. Montanari, C. Parascandolo, K. E. Rehm, F. Scarlassara, S. Szilner, X. D. Tang, and C. A. Ur, Effects of transfer channels on near- and sub-barrier fusion of $^{32}S + {}^{48}Ca$, Phys. Rev. C **87**, 014611 (2013).

[21] G. Montagnoli, A. M. Stefanini, C. L. Jiang, K. Hagino, F. Galtarossa, G. Colucci, S. Bottoni, C. Broggini, A. Caciolli, P. Colovic, L. Corradi, S. Courtin, R. Depalo, E. Fioretto, G. Fruet, A. Gal, A. Goasduff, M. Heine, S. P. Hu, M. Kaur *et al.*, Fusion hindrance for the positive Q-value system $^{12}C + {}^{30}SI$, Phys. Rev. C **97**, 024610 (2018).

[22] A. Gavron, Statistical model calculations in heavy ion reactions, Phys. Rev. C **21**, 230 (1980).

[23] K. Hagino, N. Rowley, and A. Kruppa, A program for coupled-channel calculations with all order couplings for heavy-ion fusion reactions, Comput. Phys. Commun. **123**, 143 (1999).

[24] O. Akyüz and A. Winther, in *Proceedings of the International School of Physics "Enrico Fermi", Varenna, Course LXXVII*, edited by R. A. Broglia and R. A. Ricci (North Holland, Amsterdam, 1981)

[25] C.-J. S. Raman and P. Tikkanen, Adopted values of B(E2)↑ and related quantities, At. Data Nucl. Data Tables **78**, 1 (2001).

[26] T. Kibédi and R. H. Spear, Reduced electric-octupole transition probabilities B(E3; $0_1^+ \to 3_1^-$)–An update, At. Data Nucl. Data Tables **80**, 35 (2002).

[27] T. Ichikawa, K. Hagino, and A. Iwamoto, Signature of smooth transition from sudden to adiabatic states in heavy-ion fusion reactions at deep sub-barrier energies, Phys. Rev. Lett. **103**, 202701 (2009).

[28] C. L. Jiang, K. E. Rehm, B. B. Back, and R. V. F. Janssens, Expectations for ^{12}C and ^{16}O induced fusion cross sections at energies of astrophysical interest, Phys. Rev. C **75**, 015803 (2007).

[29] C. L. Jiang, K. E. Rehm, B. B. Back, and R. V. F. Janssens, Survey of heavy-ion fusion hindrance for lighter systems, Phys. Rev. C **79**, 044601 (2009).

[30] G. Montagnoli, M. D. Fabbro, A. M. Stefanini, M. Heine, M. Rocchini, E. Pilotto, G. Andreetta, D. Stramaccioni, S. Courtin, G. Colucci, B. Million, E. Monpribat, R. Depalo, B. G. Servin, M. Polettini, I. Zanon, K. Rezynkin, M. Mazzocco, A. Bonhomme, A. Trzcinska *et al.*, Recent data on fusion far below the barrier for $^{12}C + {}^{28}Si$, V International Conference on Nuclear Structure and Dynamics NSD2024, Valencia, Spain, 27–31 May 2024 [EPJ Web. Conferences (to be published)].